Anomalous Small-Angle X-ray Scattering from Nickel-Neutralized Ionomers. 2. Semicrystalline Polymer Matrices

Richard A. Register† and Stuart L. Cooper*

Department of Chemical Engineering, University of Wisconsin, Madison, Wisconsin 53706.
Received February 28, 1989; Revised Manuscript Received May 12, 1989

ABSTRACT: The ability of anomalous small-angle X-ray scattering (ASAXS) to determine the sign of the electron density difference between the crystalline and amorphous phases in a nickel-neutralized poly(ethylene-*co*-methacrylic acid) ionomer has been demonstrated. The only a priori knowledge required is which of the phases causing the reflection has a greater concentration of nickel. All observed features of the scattering patterns are consistent with the generally accepted three-phase model incorporating lamellar crystallites, interlamellar amorphous polymeric material, and ionic aggregates distributed within the amorphous lamellae. The change in the intensity of the low-q reflection was in reasonable agreement with that calculated from experimental values of f' for Ni metal. A nickel-neutralized Nafion perfluorosulfonate ionomer was also studied, but no ionomer peak was visible due to a fortuitous equality of ionic aggregate and amorphous polymer electron densities.

I. Introduction

Small-angle X-ray scattering (SAXS) is an extremely versatile tool for probing the morphology of multiphase materials and as such has found wide application in the study of semicrystalline polymers,[1] block[2] and segmented[3] copolymers, polymer blends,[4] and ionomers.[5,6] Its versatility stems from two factors: first, the wavelength and angular range match the sizes of the heterogeneities typically found in these materials, and second, there is usually a satisfactory contrast, arising from the electron density difference(s) between the phases. The contrast can be due simply to mass density differences, as in the case of semicrystalline homopolymers, or more generally, to a combination of composition and density differences. In combination with a suitable model of the structure, it is possible to extract the values of the electron density difference(s). An example of a simple model would be a two-phase lamellar system with sharp phase boundaries, where the electron density difference can be found directly from the SAXS invariant if the volume fraction of one phase is known.

Ordinarily, SAXS is performed at a fixed wavelength, typically Cu Kα (8042 eV) from an X-ray tube or rotating anode source. While such a SAXS pattern can (in combination with the correct model) yield the magnitude of an electron density difference, it cannot yield the sign—that is, it cannot reveal which phase has the greater electron density difference. The light-scattering analogue of this statement is known as Babinet's reciprocity principle.[7] As an example, a porous silica, with the pores filled with water, should exhibit the same scattering pattern as an aqueous silica suspension, provided that the pores in the first case had the identical shape, size distribution, volume fraction, arrangement, and interfacial structure as the suspended silica particles in the latter case. Mathematically, this situation arises because the SAXS intensity is proportional to the *square* of the electron density difference.

The reciprocity principle is often a hindrance when structural studies are undertaken. In some materials, such as ionomers, the composition of one phase (the ionic aggregates) is not known exactly. If a material contains more than two phases, the situation can become quite complex. If the sign as well as the magnitude of the electron density difference causing a small-angle reflection could be determined, it would make it easier to attribute that reflection to a morphological feature. Also, if the correct model is not known, sometimes only the sign is necessary to discriminate between proposed models.

Contrast variation is easier to achieve in small-angle neutron scattering (SANS), as the coherent neutron scattering length density varies irregularly with atomic number and also varies with isotope. A series of experiments may be performed where the contrast is varied, either by isotopic substitution or by systematic addition of a third component to one phase. In the case of ionomers,[8,9] deuterated water may be added, which is taken up preferentially by the ionic aggregates. Unfortunately, this method can also alter the morphology if the water content is appreciable[6] and thus is of limited utility. An ideal method of contrast variation would selectively alter the scattering power of a single phase in a known way, leaving that of the other phases unchanged. Preferably, a single sample could be used for all measurements, thus eliminating any chance for a mismatch in morphologies between samples prepared to have different contrasts. In favorable cases, resonant or anomalous SAXS (ASAXS) meets these requirements.

As described in the preceding paper, when an absorption edge of an element is approached from lower energy, the element's scattering power is decreased. Thus, the effective electron density of phases containing this element will diminish, while phases not containing the element will be unaffected. This allows for a straightforward determination of the sign of the electron density difference, provided only that it is known which phase contains the element in greater concentration. If the phase more concentrated in the element of interest has a greater electron density than neighboring phases, the scattered intensity should diminish as the absorption edge is approached. Conversely, if the phase containing the element has a smaller electron density, then further diminution of that phase's effective electron density near the edge will cause the scattered intensity to increase. ASAXS has been used in this manner to determine the composition of Guinier–Preston zones in an Al–Zn alloy[10] and of the heterogeneities in a hydrogenated CuTi alloy.[11] The only applications of ASAXS to solid polymers reported

* To whom correspondence should be addressed.
† Present address: Department of Chemical Engineering, Princeton University, Princeton, NJ 08544.

0024-9297/90/2223-0318$02.50/0

to date[12,13] have dealt with ionomers having amorphous polymer matrices, which are two-component systems. The present report extends these results to an ionomer with a semicrystalline matrix—a three-phase, three-component system (crystalline repeat units, amorphous repeat units, and ionic repeat units)—and demonstrates how ASAXS can be used to determine the signs of the electron density differences between these phases.

For this first series of experiments, we have focussed on an ionomer whose morphology has already been studied in some detail: a partially neutralized poly(ethylene-*co*-methacrylic acid), marketed as Surlyn by Du Pont. Extensive SAXS data[14-21] and suggested models[14,17,19,21] will form a valuable base against which to compare the current ASAXS data. The test specimen was partially neutralized with Ni^{2+}, whose K absorption edge (8332.8 eV for metal) lies in an easily accessible energy range with current synchrotron X-ray sources. The choice of cation does not significantly alter the morphology relative to those cations more commonly used (Na^+ and Zn^{2+}), as shown below. In addition, an attempt was made to study Nafion perfluorosulfonate ionomers.

II. Experimental Section

A. Sample Preparation. The acid form of poly(ethylene-*co*-methacrylic acid) was provided by Du Pont along with its composition: 11.2 wt % methacrylic acid, which equates to 3.95 mol % or an equivalent weight of 770 g/equiv. Material from the same lot has been the subject of previous investigations from our laboratory.[18-20] Most studies of Surlyns and similar materials have been carried out on samples neutralized with alkali metals, since their hydroxides are soluble in methanol and a single-phase solution of the copolymer and neutralizing agent in a mixed organic solvent can be achieved. Commercially, neutralization of such materials with Zn^{2+} is accomplished by milling an excess of ZnO into the melt,[22] which generally leads to incomplete reaction[23] and a suspension of residual ZnO. Since this would severely contaminate the SAXS results, a homogeneous solution method was sought. Solid polymer sufficient to produce a 0.5% w/w solution, as well as the stoichiometric amount of nickel acetate tetrahydrate, were added to mixed xylenes/dimethyl sulfoxide (4:1 v/v). Most of the polymer and some of the nickel acetate dissolved in the solution at its boiling point, as evidenced by the solution's green color. However, some residual nickel acetate, apparently bound together with some undissolved polymer, remained at the bottom of the flask, even after the solution was refluxed for 1 h. This agglomerate was removed, the xylenes were distilled off, and the homogeneous solution was allowed to cool, whereupon the dissolved material precipitated from solution. The material had the characteristic green color of Ni^{2+}. To determine the actual content of Ni^{2+} in the material, the change in X-ray absorbance at the nickel K-edge was used, as described in the preceding paper;[13] the nickel content equates to 47% neutralization. The specimen examined by ASAXS and DSC was prepared by compression molding at 190 °C and 9000 psi for 5 min, followed by quenching to room temperature. A similar sample of the acid copolymer was prepared at 160 °C.

Nafion 125 perfluorosulfonate ionomer was obtained in the form of a 5-mil film from Du Pont. Nafion is a copolymer of tetrafluoroethylene and perfluoropropylene oligomers (1–3 units) containing a tetrafluoroethylene group at one end and a sulfonic acid group at the other.[24] Nafion 125 has an equivalent weight of 1200 g/equiv and was in the acid form as provided. The film was fully hydrated before neutralization by boiling in deionized water for 30 min. A portion of this film was then neutralized by soaking in an aqueous solution of 0.2 M nickel acetate tetrahydrate for 72 h. In an attempt to further enhance the scattering power of the ionic aggregates, the sample was then exposed to NH_3 vapor by suspending it over aqueous NH_4OH (29.2 wt %) for 24 h. In a previous investigation[25] of iron-neutralized Nafion, this treatment caused the precipitation of the metal hydroxide within the ionic aggregates by complexation between the sulfonic acid groups and the NH_3. The NH_3-treated specimen was then reimmersed in the 0.2 M nickel acetate solution for 72 h. This specimen, as well as a hydrated acid sample, was dried under vacuum at 110 °C for 24 h. Some discoloration of the acid sample was noticed, while the neutralized sample remained green. It is likely that specimens dried in this fashion still contain appreciable bound water;[26,27] the dried, neutralized film was 16% thicker than the dried acid film. By measuring the jump in the X-ray absorbance at the nickel K-edge, the neutralized sample was found to contain Ni^{2+} at 114% of stoichiometric, indicating that the NH_3 treatment had little effect in this case.

B. Data Collection and Treatment. The ASAXS data were collected on Beamline II-2 at the Stanford Synchrotron Radiation Laboratory using the SSRL Biotechnology Camera[28] and were analyzed as described in the preceding paper.[13] The Surlyn specimens should exhibit isotropic scattering, as they were compression-molded in the melt. Nafion films are known[29] to have some anisotropy in the orientation of their crystallites, due to drawing during fabrication; the Nafion specimens were examined with the machine direction parallel to the detection direction (i.e., the scattering patterns are meridional). This direction was selected so that the crystallite reflection at $q = 0.40$ nm^{-1} would be clearly visible. The momentum transfer vector magnitude $q = (4\pi/\lambda) \sin \theta$, where λ is the wavelength of the radiation and 2θ is the scattering angle. Unfortunately, beam time constraints allowed the collection of the scattering pattern for the neutralized Nafion at only one sample-to-detector distance, so the maximum q available was 3.3 nm^{-1}.

The difference pattern for the neutralized Surlyn was constructed in similar fashion to those in the preceding paper.[13] SAXS patterns were collected at 49 and 4 eV below the measured absorption edge in the material. The contributions from fluorescence and resonant Raman scattering[10,30] were eliminated by matching the tails of the scattering patterns between 5.0 and 5.2 nm^{-1}, where the anomalous dispersion effects are smallest. The −4 eV pattern was then subtracted from the −49 eV pattern to yield the difference pattern. This forces the intensity in the difference pattern to be zero between 5.0 and 5.2 nm^{-1}.

Differential scanning calorimetry (DSC) thermograms were collected over the range −70 to 220 °C on a Perkin-Elmer DSC-II interfaced to a TADS data station. Indium and mercury were used as temperature calibration standards, with the heat of fusion of the former being used for enthalpy calibration. The sample weights used were 15 ± 1 mg. The materials were quenched from room temperature to −80 °C at 320 °C/min and then scanned at 20°C/min. The melting enthalpies were calculated by drawing a base line between 22 and 130 °C.

III. Results and Discussion

While the morphology of Surlyn and similar materials was initially the subject of much debate,[5] it is now generally accepted that the material comprises lamellar crystallites which resemble those in low-density polyethylene (LDPE, electron density ρ_2), an amorphous polymer phase consisting of ethylene and methacrylic acid units and perhaps unaggregated methacrylate residues (ρ_0), and ionic aggregates consisting of a mixture of ionic and polymeric material (ρ_1) dispersed within the amorphous polymer phase. A schematic diagram of the morphology is shown in Figure 1. Two electron density profiles are shown for the ray tracing across the center of the figure. At the top is the profile seen at length scales comparable to the thickness of the crystallites, i.e., at low q; at the bottom, the profile is that seen at length scales comparable to the diameter of the ionic aggregates, i.e., at high q. Thus, depending on the size scale of interest, the material can appear to have two or three phases. The "amorphous phase" seen at the larger length scale has an electron density ρ_a that is the volume-fraction-weighted average of ρ_1 and ρ_0.

The morphology portrayed in Figure 1 is supported by transient[31,32] and dynamic[33,34] mechanical, birefrin-

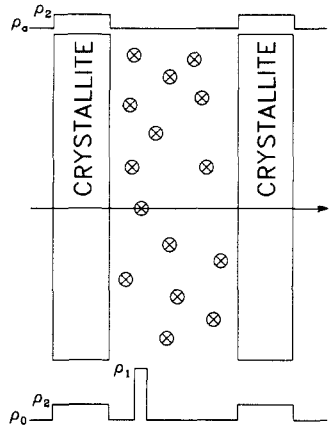

Figure 1. Morphological model for Surlyn. Center: pictorial representation; the ionic aggregates are represented by ⊕. Top: electron density profile along ray at center of diagram, seen at length scales comparable to size of crystallites. Bottom: same as at top, but on length scales comparable to size of aggregates.

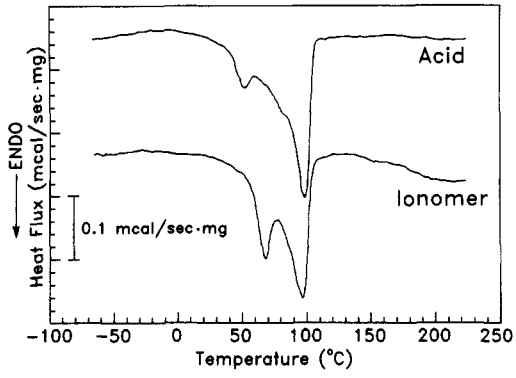

Figure 2. DSC traces for acid (top) and neutralized (bottom) Surlyn.

gence,[35] infrared dichroism,[36-38] static[39] and dynamic[40] light scattering, wide-angle X-ray scattering,[14,16,18-20,41] and SAXS[14-21] studies, among others. For low methacrylic acid contents, where this morphology is expected to apply, the electron densities are expected to obey the relations $\rho_1 > \rho_2 > \rho_0$. The relationship between ρ_2 and ρ_a is less clear. For very low ion contents, the material resembles LDPE, where $\rho_2 > \rho_a$. As the ion content is increased, however, the volume fraction of ionic aggregates increases and eventually $\rho_a > \rho_2$. SAXS patterns acquired at a single energy cannot reveal whether ρ_a or ρ_2 is larger. Part of the purpose of this report is to show that ASAXS can answer this question.

For Nafion, a morphology similar to that shown in Figure 1 is expected, though the degree of crystallinity may be much higher and the order of the electron densities is less clear. Because of the considerable difference in size between the crystalline lamellae and the ionic aggregates, both Surlyn and Nafion can exhibit two resolvable SAXS reflections. The peak at lower q, less than 1 nm^{-1}, is similar to that occurring in semicrystalline homopolymers due to scattering between lamellae (contrast between ρ_2 and ρ_a). The peak at higher q, typically 1.5–3.5 nm^{-1}, is due to scattering involving the ionic aggregates (contrast between ρ_1 and ρ_0). For brevity of notation, these peaks will be referred to as the "crystallite" and "ionomer" peaks, respectively.

A. Surlyn Samples. Differential scanning calorimetry results for the two Surlyn samples are shown in Figure 2. The traces are similar to those reported before[18-20,42] for similar materials and show a wide melting range. Since the material is a random copolymer, it should have a broad

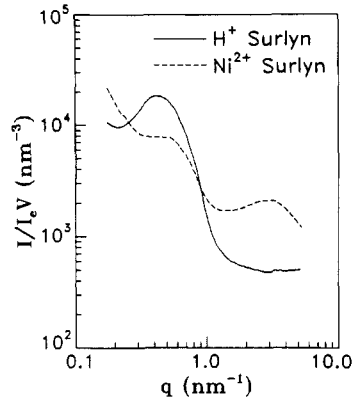

Figure 3. Scattering patterns for (—) acid Surlyn and (- - -) neutralized Surlyn, both taken at 49 eV below the measured nickel K-edge in the ionomer.

Table I
Morphological Parameters for Surlyns and Nafions

sample	final mp, °C	w_c	ϕ_c	long spacing, nm
acid Surlyn	98.3	0.33	0.30	11.0
neutralized Surlyn	96.3	0.32	0.29	10.1
acid Nafion				10.8
neutralized Nafion				11.2

distribution of ethylene sequence lengths, which could lead to a distribution of lamellar thicknesses and melting points. Also, Surlyns are very slow to crystallize compared with LDPE,[18,39] and thus many of the lamellae in these quenched samples would likely thicken with annealing to produce a narrower melting range.[18] The weight fraction of crystallinity w_c was estimated by using a value of $\Delta H = 67$ cal/g for 100% crystalline polyethylene;[43] w_c is nearly the same for the acid and ionomer samples, as has been reported previously[18-20] and is approximately 30%. Table I contains a summary of the DSC results.

Scattering patterns for the acid and ionomer, taken at 49 eV below the measured nickel K-edge in the ionomer, are shown in Figure 3. The acid shows a single reflection quite similar to that observed in LDPE.[1,44] In the ionomer, the intensity of this reflection is lower by a factor of 2, even though the level of crystallinity is the same. This is consistent with incorporation of Ni^{2+} into the "amorphous phase", which changes $(\rho_2 - \rho_a)$. The interlamellar distance, or "long spacing", is obtained from the Bragg spacing of the peak in a plot of $q^2(I/I_eV)$ vs q; the long spacings, listed in Table I, are quite similar for the acid and ionomer. The ionomer scattering pattern in Figure 3 also shows the "ionomer peak", located at 3.2 nm^{-1}, and the characteristic upturn at zero angle, which were discussed in the previous paper.

Figure 4 shows scattering patterns for the ionomer, taken at 49 and 4 eV below the edge. The background level increases near the edge due to the isotropic contribution of fluorescence and resonant Raman scattering.[10,30] After this background is subtracted, the curves in Figure 4 reveal that the ionomer peak diminishes in height, consistent with the expected decrease in ρ_1 due to the attenuation of the scattering power of the Ni^{2+} ions near the edge. Simultaneously, the crystallite peak near 0.6 nm^{-1} increases in intensity. This effect is made clearer in Figure 5, which shows the difference pattern constructed from the two patterns in Figure 4 (higher energy minus lower energy). The difference pattern exhibits, in order of increasing q, an upturn, a negative-going crystallite peak, and the ionomer peak. This clearly shows that, on going from 49 to 4 eV below the edge, $(\rho_1 - \rho_0)^2$ decreases, while $(\rho_2 - \rho_a)^2$ increases. Since the primary effect of changing the energy

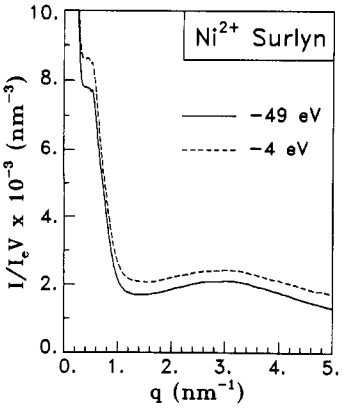

Figure 4. Neutralized Surlyn: -49 eV (—) and -4 eV (- - -) patterns. Note isotropic intensity contributions from fluorescence and resonant Raman scattering.

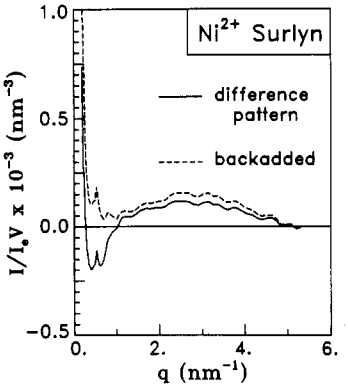

Figure 5. Difference patterns for neutralized Surlyn: difference pattern of curves in Figure 4 (—) and same with 0.045 times the -49 eV pattern added (- - -).

is to lessen ρ_1 and thereby lessen ρ_a, this conclusively proves that $\rho_2 > \rho_a$ for this specimen.

The importance of the results in Figure 5 are that they show the power of ASAXS to determine the sign of an electron density difference, knowing only which phase is richer in the element of interest, which can aid in assigning a morphological origin to an observed reflection. For example, in the present case, if we knew that the material contains both crystallites and ionic aggregates but did not know which of these caused which reflection, the difference pattern in Figure 5 would immediately lead us to the correct conclusion.

The SAXS pattern for a neutralized Surlyn is essentially a superposition of scattering involving the ionic aggregates and scattering involving the lamellae because of their difference in size. Each of these two components will be affected differently as the X-ray energy is changed. Thus, it is conceivable to use the -49 and -4 eV patterns in Figure 4 to form linear combinations that reflect *only* scattering between the lamellae *or* between the aggregates but not both. This goal was the original motivation for these experiments. An example is shown as the dashed curve in Figure 5, which is the result of adding 0.045 times the -49 eV pattern (with background subtracted so as to set the intensity equal to zero at 5.2 nm^{-1}) to the difference pattern. (Alternatively, this may be thought of as subtracting the -4 eV pattern from 1.045 times the -49 eV pattern.) The dashed curve in Figure 5 could be used, in principle, to extract morphological parameters related to the ionic aggregates, in combination with an appropriate morphological model.[6] However, because the ionomer peak in Surlyn occurs at a larger q value than for most ionomers and is quite broad and because the level of background intensity to add to the dashed curve in Figure 5 is uncertain,[13] accurate values of model parameters cannot be reliably extracted from the data without having a wider q range available.

The value 0.045 was determined visually as the amount required to eliminate the crystallite peak, producing a SAXS pattern which resembles that from amorphous ionomers. This indicates that there was approximately a 4.5% change in $(\rho_2 - \rho_a)^2$ on going from 49 to 4 eV below the edge. A reasonable question to ask, then, is how well does this value of 4.5% agree with the value calculated from the known compositions and the measured f' values for Ni metal? With perfect knowledge of the domain compositions and structure, this value should be calculable a priori. However, our incomplete knowledge requires that we follow a more circuitous route. Assuming all Ni^{2+} is contained in the amorphous phase and knowing the material's composition and the f' values for Ni^0 at the two energies, we can easily estimate the change in the effective electron density difference between the crystallites and amorphous interlamellar regions. This can be converted to a change in the intensity of the crystallite reflection, provided the electron density difference at one energy is known. It is in determining this latter quantity that substantial calculation is involved, since this first requires an estimate of the diffuse boundary thicknesses between the crystallites and amorphous regions.

For a semicrystalline homopolymer with crystalline volume fraction ϕ_c and sharp phase boundaries, the electron density difference can be calculated from the SAXS invariant[45] Q:

$$Q = \int_0^\infty q^2(I/I_eV)\,dq = 2\pi^2(\rho_2 - \rho_a)^2\phi_c(1 - \phi_c) \quad (1)$$

Since the neutralized Surlyn is a three-phase system and neither the neutralized nor acid Surlyn would be expected to have sharp phase boundaries, this equation must be applied judiciously. First, the acid Surlyn SAXS pattern was examined; the only corrections to eq 1 that apply for this material are that the background intensity must first be subtracted and the diffuse boundaries accounted for. A Vonk-like[46] background of the form

$$(I/I_eV)_b = A + Bq^4 \quad (2)$$

was fit to the data at high q. The remaining scattered intensity was modelled by Porod's law,[47] including a sigmoidal boundary produced by a Gaussian smoothing function[48,49] with a standard width σ:

$$I/I_eV = (I/I_eV)_b + Kq^{-4}e^{-(\sigma q)^2} \quad (3)$$

The range of fit used was selected based on Ruland's suggestion[50] that the minimum q at which Porod's Law should hold is twice the value of the peak position, where only a single peak is evident. The interfacial thickness parameter σ was found to be 0.22 nm for acid Surlyn; however, several workers have commented on the difficulties in extracting phase boundary thicknesses from SAXS measurements.[49,51,52] This value may be compared with those for poly(ethylene-*co*-vinyl acetate)s of similar comonomer content and crystallinity, as vinyl acetate is an isomer of methacrylic acid. Using the relation between the width of a linear gradient, $E = (12)^{1/2}\sigma$, Vonk and Pijpers[44] found an average value of $\sigma = 0.39$. Correcting for the diffuse phase boundaries[49] and extrapolating to zero and infinite q, the invariant found for the acid Surlyn was 2940 nm^{-6}. The w_c values found by DSC were converted to ϕ_c fractions by using the parameters determined by Marx[18] and are listed in Table I; from

the value of Q, a value of $(\rho_2 - \rho_a)$ of 26.6 e/nm^3 results. For pure polyethylene, this value is about 49.5 e/nm^3. If the acid Surlyn is assumed to consist of pure polyethylene crystallites and amorphous domains that are ideal mixtures of ethylene and methacrylic acid units, this value should be 34.9 e/nm^3, giving a calculated Q = 5050 nm^{-6}. The discrepancy between this value and that observed experimentally is far greater than can be accounted for by errors in determining σ; for example, if σ = 0.39 nm is used, the experimental Q = 3170 nm^{-6}. This strongly suggests that some methacrylic acid units are incorporated in the crystallites, where they act as defects and lower the electron density; this has been demonstrated for poly(ethylene-*co*-vinyl acetate)s.[44]

In determining $(\rho_2 - \rho_a)$ for the neutralized Surlyn, we have the additional complication of scattering from the ionic aggregates. For eq 1 to be valid, not only must the background scattering be subtracted, but also the scattering from the ionic aggregates. This is a difficult proposition and is the major source of error in the calculations. The ionomer peak region was fit to the Yarusso model plus a constant background, as described in the previous paper;[13] this was then subtracted from the data.

Also, the diffuse boundary thickness cannot be determined directly for the Ni^{2+} Surlyn because the ionomer peak lies in the Porod region for the crystallite peak, and the subtraction procedure discussed above is not highly accurate. As shown above, however, the value of Q is not very sensitive to the value of σ, and thus the value of $(\rho_2 - \rho_a)$ will not be either. Therefore, the diffuse boundary thickness was assumed to be the same as in the acid Surlyn, and the Porod constant K determined for the acid Surlyn was adjusted by assuming that K is inversely proportional to the long spacing (which is inversely proportional to the surface-to-volume ratio for a lamellar structure[44]) and to the invariant Q. The data were truncated at 1.4 nm^{-1} and Porod's law used to extrapolate to infinite q. This procedure yielded a value of 1450 nm^{-6} for the invariant at 49 eV below the edge or a value of $(\rho_2 - \rho_a)$ of 18.9 nm^{-3}.

On the basis of the the data of Suortti et al.,[53] f' for Ni metal is −4.50 e at 49 eV below the edge and −6.61 e at 4 eV below. On the basis of an assumed density of the amorphous phase[18] of 0.92 g/cm^3 and with the assumption that all nickel ions reside in the amorphous phase, ρ_a should drop by 0.56 e/nm^3 between these two energies. This would, in turn, lead to an increase in the crystallite peak intensity of 6.2%. This should be considered reasonable agreement with the 4.5% determined visually in Figure 5. This procedure suggests that, with data of sufficiently high quality (both in accumulated counts and in q range), it is possible to use ASAXS to construct ionomer scattering patterns containing only a single reflection, by suitable linear combination of scattering patterns (containing multiple reflections) taken at different energies.

B. Nafion Samples. The scattering patterns at 50 eV below the measured Ni^{2+} K-edge are shown in Figure 6, for both the acid and neutralized Nafion. These patterns are largely similar to meridional patterns reported previously.[29] The acid Nafion shows two prominent features, a crystallite peak at 0.40 nm^{-1} and an "ionomer" peak at 2.2 nm^{-1}. In contrast to Surlyn, the acid groups in Nafion are thought to form their own microdomains,[29,54] analogous to the ionic aggregates in neutralized Nafion. This difference is most likely due to the much stronger polarity and acid character of sulfonic acid groups in comparison with carboxylic acid groups; the ionomer peak has been observed for the acid form of sulfonated polystyrene as well.[6,13] The neutralized Nafion exhibits a crystallite reflection at a reduced intensity relative to the acid; the ionomer peak is not visible.

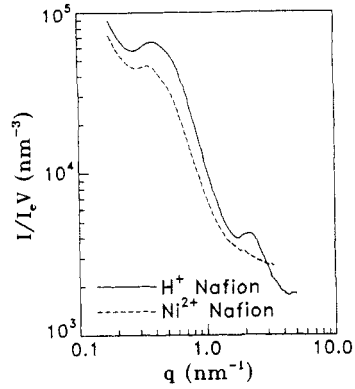

Figure 6. Scattering patterns for (—) acid Nafion and (- - -) neutralized Nafion, both taken at 50 eV below the measured nickel K-edge in the ionomer.

The difference in intensity of the crystallite peak between the acid and ionomer patterns arises from the same source as in the Surlyns; the incorporation of nickel into the amorphous phase serves to increase ρ_a and thus lower $(\rho_2 - \rho_a)^2$ if $\rho_2 > \rho_a$. However, the ionomer peak behaves oppositely to that observed in Surlyn; it is present in the acid but absent in the ionomer. Many SAXS studies[9,29,54] on Nafion samples neutralized with cations other than Ni^{2+} have observed the ionomer peak within the q range shown in Figure 6, so it is unlikely that the ionomer is void of ionic aggregates. More likely, there is a fortuitous equality between the electron densities of the amorphous poly(tetrafluoroethylene) (ρ_0) and the ionic aggregates (ρ_1). On the basis of a mass density[55] of 2.00 g/cm^3, amorphous PTFE should have an electron density of 578 e/nm^3, compared with 294 e/nm^3 for amorphous polyethylene. Thus, the most likely explanation for the behavior of the ionomer peaks in Figure 6 is that, in the acid form, $(\rho_1 - \rho_0)$ is negative, while in the neutralized form it is approximately zero. This observation directly yields an estimate of the electron density of the ionic aggregates, which may be useful in testing the validity of structural models of the aggregates. For comparison, the effective electron density of $Ni(CH_3COO)_2 \cdot 4H_2O$ at 49 eV below the edge is about 546 e/nm^3. Unfortunately, the absence of an ionomer peak in the neutralized form, plus the high X-ray absorbance of Nafion, made a difference pattern analysis similar to that performed for Surlyn impossible.

Some of the advantages of the ASAXS technique have been demonstrated in this report—in particular, it has been shown how ASAXS experiments can determine the sign of the electron density difference causing an observed reflection. An obvious limitation of the method, however, is that it requires that an element with accessible absorption edges be present in the material. With current monochromator designs, this translates to elements with atomic numbers greater than about 20. However, this does not mean the method is limited to the study of ionomers. For instance, bromine and iodine lie within this range, as do some of the dopants used in conducting polymers.[56] Also, the technique of heavy-metal staining is often used in electron microscopy;[57] similarly, specimens for ASAXS could be "stained" by adding heavy atoms to particular phases in the material.

IV. Conclusions

The ability of ASAXS to determine the sign of the electron density difference causing an observed reflection has

been demonstrated for a nickel-neutralized Surlyn ionomer. All observed features of the scattering pattern were consistent with the generally accepted three-phase morphological model, incorporating lamellar crystallites, interlamellar amorphous polymeric material, and ionic aggregates residing within the amorphous layers. The change in the "crystallite" peak intensity was found to be 4.5% on going from 49 to 4 eV below the nickel K-edge; the calculated value, based on f' from nickel metal, is 6.2%. Specimens of acid and nickel-neutralized Nafion were also examined; again, the results were consistent with the three-phase model, with the aggregates in the acid form having a lower electron density than the amorphous polymer surrounding them. The absence of a peak in the neutralized Nafion is attributed to a fortuitous cancellation between the electron densities of the aggregates and the amorphous PTFE regions; this yields an electron density of approximately 580 e/nm^3 for the aggregates.

Acknowledgment. R.A.R. wishes to thank Prof. Keith O. Hodgson for the opportunity to conduct these ASAXS experiments, using the SSRL Biotechnology Camera. The assistance of Drs. Stevan R. Hubbard and Soichi Wakatsuki was invaluable in setting up the camera and collecting and transferring the data, and they provided many helpful discussions as well. Y. S. Ding also assisted in the data collection. The Nafion 125 membrane was generously provided by Drs. William Y. Hsu and Louis L. Burton of E. I. duPont de Nemours and Co. Support for this work was provided by the U.S. Department of Energy through Grant DE-FG02-88ER45370; by the donors of the Petroleum Research Fund, administered by the American Chemical Society; and by a fellowship for R.A.R. from the Fannie and John Hertz Foundation. The Stanford Synchrotron Radiation Laboratory is supported by the Department of Energy, Office of Basic Energy Science, and the National Institutes of Health, Biotechnology Resources Program, Division of Research Resources.

Registry No. Nafion 125, 65506-90-3; (ethylene)(methacrylic acid)·XNi (copolymer), 76522-87-7.

References and Notes

(1) Schultz, J. M. *Makromol. Chem. Macromol. Symp.* **1988**, *15*, 339.
(2) Hashimoto, T.; Shibayama, M.; Kawai, H. *Macromolecules* **1980**, *13*, 1237.
(3) Tyagi, D.; McGrath, J. E.; Wilkes, G. L. *Polym. Eng. Sci.* **1986**, *26*, 1371.
(4) Russell, T. P.; Hadzioannou, G.; Warburton, W. *Macromolecules* **1985**, *18*, 78.
(5) MacKnight, W. J.; Earnest, T. R. *J. Polym. Sci., Macromol. Rev.* **1981**, *16*, 41.
(6) Yarusso, D. J.; Cooper, S. L. *Macromolecules* **1983**, *16*, 1871.
(7) Babinet, M. *C. R. Hebd. Seances Acad. Sci.* **1963**, *56*, 411.
(8) Roche, E. J.; Stein, R. S.; MacKnight, W. J. *J. Polym. Sci., Polym. Phys. Ed.* **1980**, *18*, 1035.
(9) Roche, E. J.; Pinéri, M.; Duplessix, R.; Levelut, A. M. *J. Polym. Sci., Polym. Phys. Ed.* **1981**, *15*, 1390.
(10) Goudeau, P.; Fontaine, A.; Naudon, A.; Williams, C. E. *J. Appl. Crystallogr.* **1986**, *19*, 19.
(11) Goudeau, P.; Naudon, A.; Chamberod, A.; Rodmacq, B.; Williams, C. E. *Europhys. Lett.* **1987**, *3*, 269.
(12) Ding, Y. S.; Hubbard, S. R.; Hodgson, K. O.; Register, R. A.; Cooper, S. L. *Macromolecules* **1988**, *21*, 1698.
(13) Register, R. A.; Cooper, S. L. *Macromolecules*, preceding paper in this issue.
(14) Wilson, F. C.; Longworth, R.; Vaughan, D. J. *Polym. Prepr. (Am. Chem. Soc., Div. Polym. Chem.)* **1968**, *9*, 505.
(15) Delf, B. W.; MacKnight, W. J. *Macromolecules* **1969**, *2*, 309.
(16) Kao, J.; Stein, R. S.; MacKnight, W. J.; Taggart, W. P.; Cargill, G. S. *Macromolecules* **1974**, *7*, 95.
(17) MacKnight, W. J.; Taggart, W. P.; Stein, R. S. *J. Polym. Sci., Polym. Symp.* **1974**, *45*, 113.
(18) Marx, C. L.; Cooper, S. L. *Makromol. Chem.* **1973**, *168*, 339.
(19) Marx, C. L.; Caulfield, D. F.; Cooper, S. L. *Macromolecules* **1973**, *6*, 344.
(20) Marx, C. L.; Cooper, S. L. *J. Macromol. Sci., Phys.* **1974**, *B9*, 19.
(21) Yarusso, D. J.; Cooper, S. L. *Polymer* **1985**, *26*, 371.
(22) Harrison, S. R.; Broughton, R. M. U.S. Patent 3 454 280, July 8, 1969, to Dunlop Rubber Co.
(23) Register, R. A.; Giroux, T. A.; Homan, J. G.; Cooper, S. L., unpublished results.
(24) Yeager, H. L; Eisenberg, A. In *Perfluorinated Ionomer Membranes*; ACS Symposium Series 187; Eisenberg, A., Yeager, H. L., Eds.; American Chemical Society: Washington, 1982.
(25) Pan, H. K.; Meagher, A.; Pinéri, M.; Knapp, G. S.; Cooper, S. L. *J. Chem. Phys.* **1985**, *82*, 1529.
(26) Duplessix, R.; Escoubes, M.; Rodmacq, B.; Volino, F.; Roche, E.; Eisenberg, A.; Pinéri, M. In *Water in Polymers*; ACS *Symposium Series* 127; Rowland, S. R., Ed.; American Chemical Society: Washington, 1980.
(27) Rodmacq, B.; Coey, J. M.; Escoubes, M.; Roche, E.; Duplessix, R.; Eisenberg, A.; Pinéri, M. In *Water in Polymers*; ACS Symposium Series 127; Rowland, S. R., Ed.; American Chemical Society: Washington, 1980.
(28) Hubbard, S. R. Ph.D. Thesis, Stanford University, 1987.
(29) Gierke, T. D.; Munn, G. E.; Wilson, F. C. *J. Polym. Sci., Polym. Phys. Ed.* **1981**, *19*, 1687.
(30) Eisenberger, P.; Platzman, P. M.; Winick, H. *Phys. Rev. B* **1976**, *13*, 2377.
(31) Ward, T. C.; Tobolsky, A. V. *J. Appl. Polym. Sci.* **1967**, *11*, 2403.
(32) Bonotto, S.; Bonner, E. F. *Polym. Prepr. (Am. Chem. Soc., Div. Polym. Chem.)* **1968**, *9*, 537.
(33) MacKnight, W. J.; McKenna, L. W.; Read, B. E. *J. Appl. Phys.* **1967**, *38*, 4208.
(34) MacKnight, W. J.; Kajiyama, T.; McKenna, L. *Polym. Eng. Sci.* **1968**, *8*, 267.
(35) Kajiyama, T.; Stein, R. S.; MacKnight, W. J. *J. Appl. Phys.* **1970**, *41*, 4361.
(36) MacKnight, W. J.; McKenna, L. W.; Read, B. E.; Stein, R. S. *J. Phys. Chem.* **1968**, *72*, 1122.
(37) Read, B. E.; Stein, R. S. *Macromolecules* **1968**, *1*, 116.
(38) Uemura, Y.; Stein, R. S. *Macromolecules* **1971**, *4*, 490.
(39) Prud'homme, R. E.; Stein, R. S. *Macromolecules* **1971**, *4*, 668.
(40) Prud'homme, R. E.; Stein, R. S. *J. Polym. Sci., Polym. Phys. Ed.* **1973**, *11*, 1347.
(41) Kajiyama, T.; Oda, T.; Stein, R. S.; MacKnight, W. J. *Macromolecules* **1971**, *4*, 198.
(42) MacKnight, W. J.; Taggart, W. P.; McKenna, L. *J. Polym. Sci. Symp.* **1974**, *46*, 83.
(43) Aggarwal, S. L. In *Polymer Handbook*, 2nd ed.; Brandrup, J., Immergut, E. H., Eds.; Wiley: New York, 1975; p V-13.
(44) Vonk, C. G.; Pijpers, A. P. *J. Polym. Sci., Polym. Phys. Ed.* **1985**, *23*, 2517.
(45) Porod, G. In *Small-Angle X-Ray Scattering*; Glatter, O., Kratky, O., Ed.; Academic Press: New York, 1982.
(46) Vonk, C. G. *J. Appl. Crystallogr.* **1971**, *4*, 70.
(47) Porod, G. *Kolloid-Z.* **1951**, *124*, 83.
(48) Ruland, W. *J. Appl. Crystallogr.* **1971**, *4*, 70.
(49) Koberstein, J. T.; Morra, B.; Stein, R. S. *J. Appl. Crystallogr.* **1980**, *13*, 34.
(50) Ruland, W. *Colloid Polym. Sci.* **1977**, *255*, 417.
(51) Roe, R. J. *J. Appl. Crystallogr.* **1982**, *15*, 182.
(52) Ruland, W. *Macromolecules* **1987**, *20*, 87.
(53) Suortti, P.; Hastings, J. B.; Cox, D. E. *Acta Crystallogr. A* **1985**, *A41*, 417.
(54) Fujimura, M.; Hashimoto, T.; Kawai, H. *Macromolecules* **1981**, *14*, 1309.
(55) Sperati, C. A. In *Polymer Handbook*, 2nd ed.; Brandrup, J., Immergut, E. H., Eds.; Wiley: New York, 1975; p V-29.
(56) Skotheim, T. A., Ed.; *Handbook of Conducting Polymers*; Marcel Dekker: New York, 1986.
(57) Sawyer, L. C.; Grubb, D. T. *Polymer Microscopy*; Chapman and Hall: New York, 1987.